

# Self-organization of a wheeled robotic swarm using virtual spring-damper mesh

Jakub Wiech

Department of Applied Mechanics and Robotics, Rzeszow University of Technology, Rzeszow, Poland

---

## Article Info

### Article history:

Received Oct 12, 2022

Revised Oct 30, 2022

Accepted Jan 5, 2023

### Keywords:

Physicomimetics

Self-organization

Virtual spring-damper mesh control

Wheeled robotic swarm

---

## ABSTRACT

The article analyzes the problem of self-organization of randomly placed wheeled robots around a stationary reference point, into a given shape of a regular polygon. The paper gives an answer to the question how virtual forces from virtual spring-damper connections between robots allow self-organization of the swarm into the desired shape. The presented method of control is described in detail with the description of  $i$ -th robot dynamics and tested numerically and experimentally. The swarm's self-organization is aimed at moving randomly spaced robots with a random frame orientation to a given distance to a reference point, reaching and maintaining a given distance between neighboring robots. The paper presents the results of numerical tests and experimental research and ends with discussion and conclusions. The paper's results could be expanded for applications related to spatial distribution of mobile robots.

*This is an open access article under the [CC BY-SA](#) license.*



---

## Corresponding Author:

Jakub Wiech

Department of Applied Mechanics and Robotics, Rzeszow University of Technology

12 Powstancow Warszawy Street, Rzeszow, Poland

Email: j.wiech@prz.edu.pl

---

## 1. INTRODUCTION

Self-organization in swarm robotics is a process that allows achieving global structures from local interactions [1]–[3]. In the literature, additional features of self-organization are presented i.e: adaptation to changing working conditions without modification of swarm structure and distribution of robots. It allows for finding an optimal solution for swarm objective or automatic modification of swarm topology when new robots are added or existing robots are taken out of the swarm [4]–[6]. A swarm has an ability to reorganize its structure or behavior without external intervention. Unfortunately it is difficult to precisely predict the behavior of a swarm in the process of self-organization [7]. In literature we can find methods of swarm control based on robot-human interactions [8], often used graph theory methods [9] or game theory [10]. In coordinated movement of a robotic swarm, the control methods relay often on virtual potential field, virtual physics or so called Physicomimetics [11]. The robots have to reach and maintain the desired distance between themselves (sometimes resulting in creation of formation) and move in coordinated manner following the desired trajectory or moving to the goal point. As examples of methods used for swarm control, similar to the idea of physicomimetics, we can distinguish: the virtual heading method, the artificial forces method and the virtual potential field method. The virtual heading is a reference by which robots are able to determine their direction relative to other robots [12]. Based on the sensors, the distance to the nearest neighboring robots and the swarm's virtual direction, the swarm is able to achieve coherent coordinated movement, maintaining the ability to avoid

obstacles without knowing the direction to the goal. In the work [13] a modification of the communication method between robots was suggested, by means of which a given heading to the target is transmitted. The method of artificial potential fields [14]–[20] is a generalization of the method of virtual forces by introducing the relationship between the value of the virtual force and the virtual potential field. The environment in which the robot is located is depicted as a sum of virtual potential fields from obstacles, other robots and the goals pursued by individual robots and swarms.

The article analyzes the problem of self-organization of randomly spaced robots around a stationary reference point into a shape of a regular polygon. The swarm's self-organization is aimed at moving randomly spaced robots with a random frame orientation to a given distance to a reference point, reaching and maintaining a given distance between neighboring robots. The presented method of control is based on virtual forces that are used to calculate the kinematic parameters of the robots.

This paper is an expansion on the method presented in the article [21] allowing for practical application of the self-organization method on a real swarm of robots. The article replaces the swarm leader with a reference point whose coordinates are known to all robots and introduces the concept of a geometrical center as a quality indicator of self-organization of the swarm. It solves a problem of modeling the behavior of a swarm based on robots used in the experiment, by describing in detail the robot dynamics as well as the swarm control method. The paper describes solutions to the application problems of the presented method. The adopted solutions are verified on a robotic arena equipped with motion capture system. The paper presents the results of numerical tests and experimental research and ends with a discussion on the obtained solutions with conclusions.

## 2. SWARM MODELING AND CONTROL

### 2.1. Single robot model

The swarm consists of two-wheeled robots with two spherical support wheels 3,4, as shown in Figure 1(a). We assume that the motion of the  $i$ -th robot takes place on a smooth surface, without slippage. The robot is driven by two DC motors as marked in Figure 1(a) as 1 and 2 with wheels marked as 7 and 6 as shown in Figure 1(b), with radius  $r$  and geometric centers marked as points B, C. The center of gravity of the robot is at point  $S_i$  on the robot frame 5. Point  $S_i$  lies on the axis of symmetry of the drive wheels at a distance  $d$  from the center of the wheel segment — CB — marked as point  $A_i$ . Rotation angles of wheels 6 and 7 were marked as  $\alpha_{1i}, \alpha_{2i}$ . Point D is the frame's instantaneous rotation center, and  $\beta_i$  is the frame's instantaneous rotation angle.

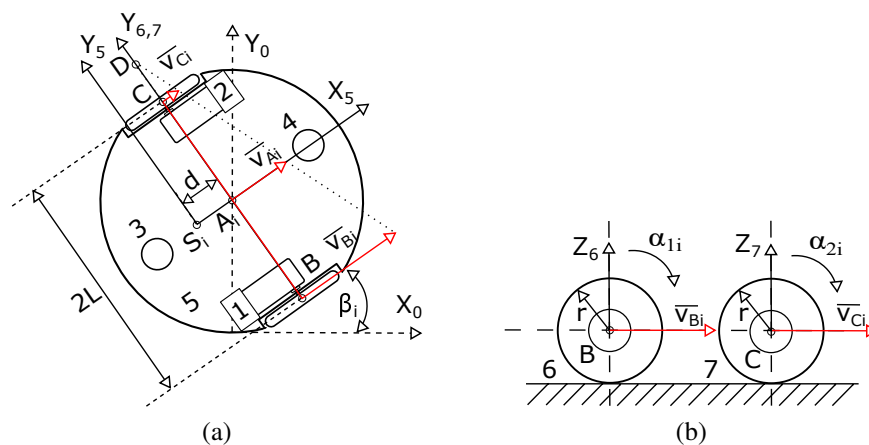


Figure 1. The schematics of the  $i$ -th wheeled robot in the swarm of robots (a) robot frame and (b) robot wheels

The  $i$ -th robot moves along a specific trajectory expressed as a function of the angular velocity of the drive wheels  $\dot{\alpha}_{1i}, \dot{\alpha}_{2i}$ . The angular velocities of the robot's driving wheels are the robot configuration coordinates, determined from the following (1):

$$\dot{\alpha}_{1i} = \frac{v_{Ai}}{r} + \dot{\beta}_i \frac{L}{r}, \quad \dot{\alpha}_{2i} = \frac{v_{Ai}}{r} - \dot{\beta}_i \frac{L}{r}, \quad (1)$$

as well as (2):

$$\begin{aligned}\dot{\beta}_i &= \frac{r}{2L}(\dot{\alpha}_{1i} - \dot{\alpha}_{2i}), & \dot{x}_{Ai} &= \frac{r}{2}(\dot{\alpha}_{1i} + \dot{\alpha}_{2i})\cos(\beta_i), \\ \dot{y}_{Ai} &= \frac{r}{2}(\dot{\alpha}_{1i} + \dot{\alpha}_{2i})\sin(\beta_i),\end{aligned}\quad (2)$$

where:  $\dot{\alpha}_{1i}, \dot{\alpha}_{2i}$  - angular velocities of driving wheels,  $r$  - radius of the robot's driving wheel,  $L$  - half the length of the robot's driving axis. Robot kinematic parameters are  $\alpha_{1i}, \alpha_{2i}, \dot{\alpha}_{1i}, \dot{\alpha}_{2i}$ .

The dynamic equation of motion of a two-wheeled robot are known in literature [22]. The adaptation of the dynamic equations for the above robot will take form:

$$M\ddot{q}_{Mi} + C(\dot{q}_{Mi})\dot{q}_{Mi} + F(\dot{q}_{Mi}) = U_i, \quad (3)$$

where:  $q_{Mi} = [\alpha_{1i}, \alpha_{2i}]^T$  - vector of generalized coordinates,  $M$  - inertia matrix,  $C(\dot{q}_{Mi})\dot{q}_{Mi}$  - vector of centrifugal and Coriolis forces,  $F(\dot{q}_{Mi})$  - vector of friction forces,  $U_i = [M_{1i}, M_{2i}]^T$  - control inputs of the  $i$ -th robot (driving torques of wheels 6 and 7).

By properly grouping matrix elements  $M, C(\dot{q}_{Mi})$  and vector  $F(\dot{q}_{Mi})$  we will have:

$$\begin{aligned}M &= \begin{bmatrix} a_1 + a_2 + a_3 & a_1 - a_2 \\ a_1 - a_2 & a_1 + a_2 + a_3 \end{bmatrix}, & F(\dot{q}_{Mi}) &= \begin{bmatrix} a_5 \operatorname{sgn}(\dot{\alpha}_{1i}) \\ a_6 \operatorname{sgn}(\dot{\alpha}_{2i}) \end{bmatrix}, \\ C(\dot{q}_{Mi}) &= \begin{bmatrix} 0 & 2a_4(\dot{\alpha}_{2i} - \dot{\alpha}_{1i}) \\ -2a_4(\dot{\alpha}_{2i} - \dot{\alpha}_{1i}) & 0 \end{bmatrix}, & U_i &= \begin{bmatrix} M_{1i} \\ M_{2i} \end{bmatrix}.\end{aligned}\quad (4)$$

The parameters vector  $a = [a_1, a_2, a_3, a_4, a_5]^T$  results from the expansion of the dynamics equations. The elements of the vector are (5):

$$\begin{aligned}a_1 &= (2m_w + m_5) \left(\frac{r}{2}\right)^2, \\ a_2 &= (2m_w L^2 + m_5 d^2 + I_{5S} + 2I_{zw}) \left(\frac{r}{2L}\right)^2, \\ a_3 &= I_{yw}, a_4 = m_5 \left(\frac{r}{2}\right)^2 \left(\frac{rd}{l^2}\right), a_5 = N_1 f_1, a_6 = N_2 f_2,\end{aligned}\quad (5)$$

where:  $m_w$  - weight of wheels 6 and 7,  $m_5$  - robot frame weight,  $I_{yw}$  - mass moment of inertia of wheel 6 about axis  $Y_6$  and wheel 7 about axis  $Y_7$  as seen in Figure 1(a),  $I_{zw}$  - mass moment of inertia of wheel 6 about axis  $Z_6$  and wheel 7 about axis  $Z_7$  as seen in Figure 1(b),  $I_{5S}$  - mass moment of inertia of the robot frame calculated with respect to the axis perpendicular to the frame and passing through point  $S_i$  as seen in Figure 1(a).

Because of the usage of drive modules with high gear ratios, we can extended the model of the  $i$ -th robot with the servomechanism model. Taking into account the dynamics equations of the robot's drive motors [23] can be written as (6):

$$\overline{M}\ddot{q}_{Mi} + \overline{C}(\dot{q}_{Mi})\dot{q}_{Mi} + \overline{F}(\dot{q}_{Mi}) = u_i, \quad (6)$$

where:

$$\begin{aligned}\overline{M} &= \begin{bmatrix} (a_1 + a_2 + a_3)r_k^2 + J_{k1} & (a_1 - a_2)r_k^2 \\ (a_1 - a_2)r_k^2 & (a_1 + a_2 + a_3)r_k^2 + J_{k2} \end{bmatrix}, \\ \overline{C}(\dot{q}_{Mi}) &= \begin{bmatrix} 0 & 2a_4 r_k^2 (\dot{\alpha}_{2i} - \dot{\alpha}_{1i}) \\ -2a_4 r_k^2 (\dot{\alpha}_{2i} - \dot{\alpha}_{1i}) & 0 \end{bmatrix}, \\ \overline{F}(\dot{q}_{Mi}) &= \begin{bmatrix} a_5 r_k^2 \operatorname{sgn}(\dot{\alpha}_{1i}) + B_1 \dot{\alpha}_{1i} \\ a_6 r_k^2 \operatorname{sgn}(\dot{\alpha}_{2i}) + B_2 \dot{\alpha}_{2i} \end{bmatrix}, & \mathbf{u}_i &= \begin{bmatrix} u_{1i} \\ u_{2i} \end{bmatrix} u_{max}, \\ u_{max} &= \frac{K_M r_k}{R} V_{max} \quad \text{for } k = 1, 2, \quad u_1, u_2 \in \langle -1, 1 \rangle.\end{aligned}\quad (7)$$

where:  $u_{1i}, u_{2i}$  - normalized control signals,  $K_M$  - torque constant,  $r_k$  - gear ratio,  $V_{max}$  - the maximum allowable voltage at the power supply input of the motors DC,  $k$  - drive module number.

In the process of parametric identification, the following values of the above parameters were obtained:  $\mathbf{a} = [7.3125 \cdot 10^{-5}, 8.97 \cdot 10^{-9}, 5.543 \cdot 10^{-6}, 0.0126, 0.917]$  and  $B_1 = 3.01 \cdot [10]^{-5}$ ,  $B_2 = 3.37 \cdot [10]^{-5}$ . From the documentations we can define other parameters:  $r = 0.03[m]$ ,  $L = 0.069[m]$ ,  $K_M = 0.048[-]$ ,  $R = 2.17[\Omega]$ ,  $r_k = 1/120[-]$ ,  $V_{max} = 7.4[V]$ . The presented model is used in simulations.

## 2.2. Swarm self-organization algorithm

The task of the robots is to reach and maintain a given distance to the reference point, while maintaining a given distance to the closest neighboring robots. Self-organization is performed for robots with random frame orientations, randomly placed around a known stationary reference point. The neighboring robots are understood as  $j$ -th robots in the sensory range of the  $i$ -th robot below a certain distance. Robots know the predefined coordinates of the reference point.

Robots can create a desired shape using only information about neighboring robots and the position of the reference point. The shapes of the swarm and kinematic parameters of robots result from the exertion of virtual forces on the  $i$ -th robot. If the value of the resultant forces acting on each robot reaches 0 or oscillates near 0, the self-organization of the swarm is considered finished. The virtual forces come from virtual spring-damper connections that link the robots to each other and to the reference point.

The behavior of the  $i$ -th robot under the influence of virtual forces can be described as shown in Figure 2. On the middle of the driving axle  $|CB|$  of the  $i$ -th robot in the swarm, a virtual force is applied from the origin point  $W_i$  of the resultant force, moving at  $\bar{v}_w$ . Point  $W_i$  is a substitute point from which the  $\bar{F}_{iW}$  is originating from Figure 2(a).

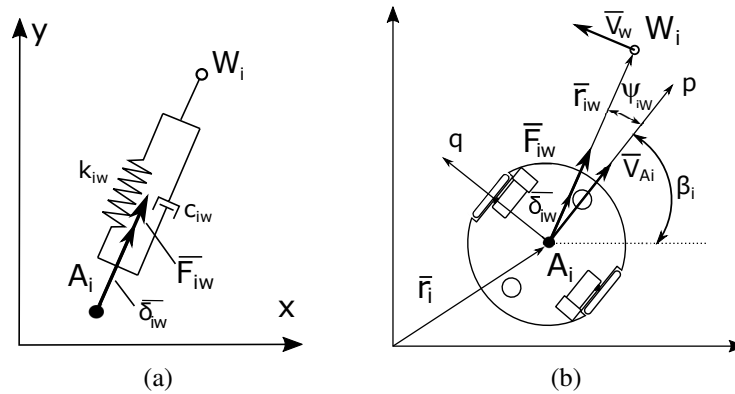


Figure 2. Swarm self-organization algorithm (a) diagram of a virtual spring and damper connecting points  $A_i$  and  $W_i$  (b) resultant virtual force acting on the  $i$ -th robot and

Virtual force  $\bar{F}_{iW}$  is a vector sum of virtual forces from neighboring robots and a reference point. The  $i$ -th robot has to move to the point  $W_i$ . The closer the distance from the point  $A_i$  to the point  $W_i$ , the closer to zero is the vector sum of the virtual forces acting on the  $i$ -th robot. The angle of inclination of the robot's frame to the  $x$  axis is  $\beta_i$ , and the center of the drive axis of the  $i$ -th robot moves at the velocity  $\bar{v}_{Ai}$  as shown in Figure 2(b).

The resultant vector  $\bar{F}_{iW}$  is can be calculated using (8):

$$\bar{F}_{iW} = (k_{iW}e_{iW} + c_{iW}\dot{e}_{iW})\bar{\delta}_{iW}, \quad (8)$$

where:  $\bar{\delta}_{iW}$  - unit vector directed from point  $A_i$  to point  $W_i$ ,  $e_{iW}$  - virtual spring deformation. The value of the vector of the resultant force acting on the  $i$ -th robot is:

$$F_{iW} = k_{iW}e_{iW} + c_{iW}\dot{e}_{iW}, \quad (9)$$

where:  $k_{iW}, c_{iW} > 0$  - spring constant of the virtual resultant spring and the damping constant of the virtual resultant damper.

The desired configuration of the  $i$ -th robot was assumed as (10):

$$q_{Wi} = [x_{Wi}, y_{Wi}, 0]^T, \quad (10)$$

whereas, the  $i$ -th robot present configuration is:

$$q_i = [x_{Ai}, y_{Ai}, \beta_i]^T, \quad (11)$$

where:  $x_{Wi}, y_{Wi}, x_{Ai}, y_{Ai}$  - coordinates of the points  $W_i$  and  $A_i$  in the stationary coordinate system, respectively. The error of the desired and final configuration of the  $i$ -th robot can be defined as (12):

$$\tilde{q}_{Wi} = q_{Wi} - q_i = [\tilde{x}_i, \tilde{y}_i, \tilde{\beta}_i]^T. \quad (12)$$

by defining the error vector  $q_{bi}$  in the polar coordinates for the  $i$ -th robot, which is under influence of the resultant force  $\overline{F_{iW}}$ , we get:

$$q_{bi} = [e_{iW}, \psi_{iW}]. \quad (13)$$

The value of  $\psi_{iW}$  angle can be determined graphically using (14):

$$\psi_{iW} = \arctg2\left(\frac{y_{Wi} - y_{Ai}}{x_{Wi} - x_{Ai}}\right) - \beta_i, \psi_{iW} \in \langle -\pi, \pi \rangle, \quad (14)$$

whereas, the deformation value  $e_{iW}$  is described by (15):

$$e_{iW} = r_{iW} = \sqrt{(x_{Wi} - x_{Ai})^2 + (y_{Wi} - y_{Ai})^2}. \quad (15)$$

In order for the robot to move in the direction of the resultant force to its source, the velocity vector of the point  $A_i$  must have the direction of the resultant vector of virtual forces acting on this robot, so the relationship must be satisfied:

$$\overline{F_{iW}} \times \overline{dV_{Ai}} = 0. \quad (16)$$

The angle  $\psi_{iW}$  between the vectors  $\overline{F_{iW}}$  and  $\overline{dV_{Ai}}$  will approach zero if the vector of the desired instantaneous angular velocity of the robot's frame  $\overline{\beta_{id}}$  is proportional and opposite to the vector product (16) [24]:

$$\overline{\beta_{id}} = -\lambda_1 (\overline{F_{iW}} \times \overline{dV_{Ai}}) \overline{k} = \overline{\omega_i}, \quad \lambda_1 > 0, \quad (17)$$

where:  $dV_{Ai}$  - infinitesimal velocity of the point  $A_i$ ,  $\overline{k}$  - unit vector on the axis perpendicular to the robot frame and passing through the point  $A_i$ .

In the  $x, y$  coordinate system we can write:

$$\overline{F_{iW}} \times \overline{dV_{Ai}} = \begin{vmatrix} i & j & k \\ F_{iWx} & F_{iWy} & 0 \\ d\dot{x}_{Ai} & d\dot{y}_{Ai} & 0 \end{vmatrix}. \quad (18)$$

The value of the desired angular velocity will take the form:

$$\overline{\beta_{id}} = -\lambda_1 (F_{iWx} d\dot{y}_{Ai} - F_{iWy} d\dot{x}_{Ai}) \overline{k}. \quad (19)$$

The values of the projections of virtual forces on the  $x$  and  $y$  axes are determined from the rotation equation of the  $p$  and  $q$  coordinate system shown in Figure 3.

$$\begin{bmatrix} F_{iWx} \\ F_{iWy} \end{bmatrix} = Rot \begin{bmatrix} F_{iWp} \\ F_{iWq} \end{bmatrix} = \begin{bmatrix} \cos\beta_i & -\sin\beta_i \\ \sin\beta_i & \cos\beta_i \end{bmatrix} \begin{bmatrix} F_{iWp} \\ F_{iWq} \end{bmatrix} = \begin{bmatrix} F_{iWp}\cos\beta_i - F_{iWq}\sin\beta_i \\ F_{iWp}\sin\beta_i + F_{iWq}\cos\beta_i \end{bmatrix}. \quad (20)$$

Projections of virtual forces on the  $p$  and  $q$  axes are (21):

$$F_{iWp} = F_{iW}\cos\psi_{iW}, \quad F_{iWq} = F_{iW}\sin\psi_{iW}. \quad (21)$$



virtual spring-damper connections between the nearest neighboring robots  $\overline{F_{ij}}$  (between points  $A_i$  and  $A_j$ ) and the reference point  $\overline{F_{ip}}$  (between point  $A_i$  and the reference point  $P$  as shown in Figure 4). Resulting vector  $\overline{F_{iW}}$  is the sum of its component vectors  $\overline{F_{ij}}$  i  $\overline{F_{ip}}$ . The vectors of virtual forces  $\overline{F_{ij}}$  i  $\overline{F_{ip}}$  are described by (30) and (31):

$$\overline{F_{ij}} = (k_{ij}e_{ij} + c_{ij}\dot{e}_{ij})\overline{\delta_{ij}}, \quad (30)$$

$$\overline{F_{ip}} = (k_{ip}e_{ip} + c_{ip}\dot{e}_{ip})\overline{\delta_{ip}}, \quad (31)$$

where  $\overline{\delta_{ij}}, \overline{\delta_{ip}}$  - unit vectors from the center of the drive axis of the  $i$ -th robot  $A_i$  to the center of the drive axis of the nearest neighboring  $j$ -th robot  $A_j$  and to the reference point  $P$  as shown in Figure 4(a), respectively.

The values of the virtual component forces are:

$$F_{ij} = k_{ij}e_{ij} + c_{ij}\dot{e}_{ij}, \quad (32)$$

$$F_{ip} = k_{ip}e_{ip} + c_{ip}\dot{e}_{ip}, \quad (33)$$

where  $k_{ij}, c_{ij} > 0, k_{ip}, c_{ip} > 0$  - the spring constant of the virtual spring and the damping constant of the virtual damper between the  $i$ -th robot and the closest  $j$ -th robot and the reference point  $P$ , respectively.

The values of the virtual deformations are expressed by (34) and (35):

$$e_{ij} = r_{ij} - l_{ij} = \sqrt{(x_{Aj} - x_{Ai})^2 + (y_{Aj} - y_{Ai})^2} - l_{ij}, \quad (34)$$

$$e_{ip} = r_{ip} - l_{ip} = \sqrt{(x_p - x_{Ai})^2 + (y_p - y_{Ai})^2} - l_{ip}, \quad (35)$$

where  $x_{Ai}, x_{Aj}, x_p \in R, y_{Ai}, y_{Aj}, y_p \in R$  -  $x$  and  $y$  coordinates of the centers of the robots  $i, j$ , and the reference point  $P, l_{ij}, l_{ip} > 0$ , respectively - resting lengths of virtual springs (the desired distances) between the  $i$ -th robot and the  $j$ -th robot and between the  $i$ -th robot and the reference point  $P$ .

The values of the derivatives of virtual deformations are as (36):

$$\dot{e}_{ij} = v_{Aj}\cos\psi_{ji} - v_{Ai}\cos\psi_{ij}, \quad (36)$$

and to the stationary reference point  $P$ ,

$$\dot{e}_{ip} = -v_{Ai}\cos\psi_{ip}, \quad (37)$$

where:  $v_{Ai}, v_{Aj} \in R$  - the velocity of the center of the driving axis of the robot  $i$  and the robot  $j$ , respectively.

The value of the angles  $\psi_{ij}, \psi_{ji}$  shown in the Figure 4(b) result from the relationship:

$$\psi_{ij} = \gamma_{ij} - \beta_i, \quad \psi_{ji} = \gamma_{ji} - \beta_j, \quad \psi_{ij}, \psi_{ji} \in \langle -\pi, \pi \rangle, \quad (38)$$

$$\gamma_{ij} = \arctg2\left(\frac{y_{Aj} - y_{Ai}}{x_{Aj} - x_{Ai}}\right), \gamma_{ji} = \arctg2\left(\frac{y_{Ai} - y_{Aj}}{x_{Ai} - x_{Aj}}\right). \quad (39)$$

The derivatives of angles  $\psi_{ij}, \psi_{ji}, \psi_{ip}$  are:

$$\dot{\psi}_{ij} = v_{Ai}\frac{\sin\psi_{ij}}{e_{ij} + l_{ij}} - v_{Aj}\frac{\sin\psi_{ji}}{e_{ij} + l_{ij}} - \dot{\beta}_i, \quad (40)$$

$$\dot{\psi}_{ji} = v_{Aj}\frac{\sin\psi_{ji}}{e_{ij} + l_{ij}} - v_{Ai}\frac{\sin\psi_{ij}}{e_{ij} + l_{ij}} - \dot{\beta}_j, \quad (41)$$

$$\dot{\psi}_{ip} = v_{Ai}\frac{\sin\psi_{ip}}{e_{ip} + l_{ip}}. \quad (42)$$

The shape of the swarm can be determined by choosing the desired distances between the robots. It is assumed that the  $i$ -th robot is affected by virtual forces only from the closest neighboring robots and from the reference point.

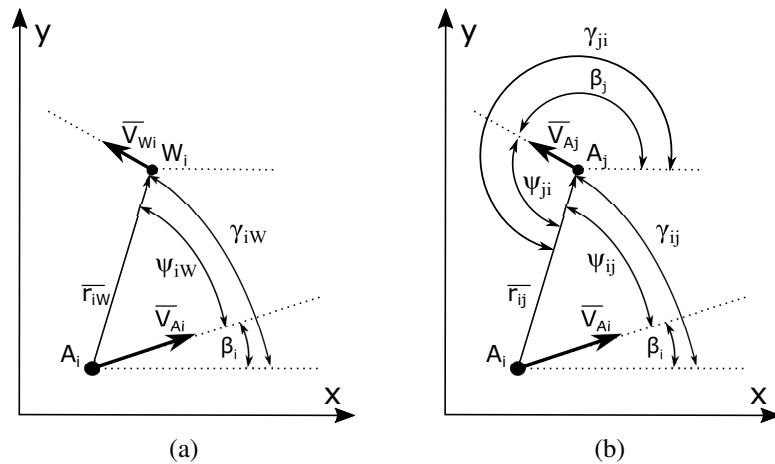


Figure 4. The relationship between the virtual forces (a) the angular relationships between the point  $A_i$  of the  $i$ -th robot and resultant point  $W_i$ , (b) the angular relationships between the centers of the robots' drive axes  $i, j$

The selection of the set distance between the robots in relation to the sensor range can be illustrated in the case of a swarm without a reference point. The forces acting on the robots will balance each other when the robots are placed at a given distance  $l_{ij}$  creating a mesh of equilateral triangles. This is the case when the robot is acted on by virtual forces that come only from the nearest neighboring robots Figure 5.

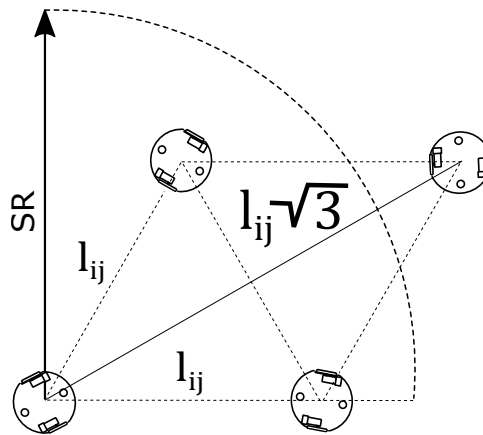


Figure 5. Robot sensor range

The range of sensors (SR) is limited to the following inequalities:

$$l_{ij}\sqrt{3} < SR < l_{ij}. \tag{43}$$

The desired trajectory of the  $i$ -th robot is realized by the tracking control algorithm. Due to the simple construction of the robot, a PD controller ("PD" block) was used as the tracking controller as shown in Figure 6. The controller gains were selected experimentally, setting the values of  $k_p = 0.113$  and  $k_d = 0.046$ . By integrating the dynamic equation of the  $i$ -th mobile robot (block "WMRi") (3), the kinematic parameters were found:  $\alpha_{1i}, \alpha_{2i}, \dot{\alpha}_{1i}, \dot{\alpha}_{2i}$ , which on the basis of (2) allow for calculation velocity projections of the point  $A_i$   $\dot{x}_{A_i}, \dot{y}_{A_i}$  and angular velocity  $\beta_i$  ("Determining WMR position" block). Knowledge of these kinematic parameters and initial conditions enables the determination of the coordinates of the  $A_i$  points and the  $\beta_i$  orientation angles of all robots. With robot kinematic parameters and reference point coordinates, based on (34)-(37), (40), (42) the deformation values  $e_{ij}, e_{ip}$ , angles  $\psi_{ij}, \psi_{ip}$  and their derivatives can be calculated (block "determining distance and orientation"). Knowing the distances, angles and their derivatives, we can

find the controls  $u_{v_i}, u_{\beta_i}$  using the (28), (29) ("controls determination" block). Based on the (1) ("kinematics equation" block) and (2) ("desired trajectory" block), the desired trajectory for the  $i$ -th robot is determined. The control scheme of the  $i$ -th swarm robot is shown in Figure 6.

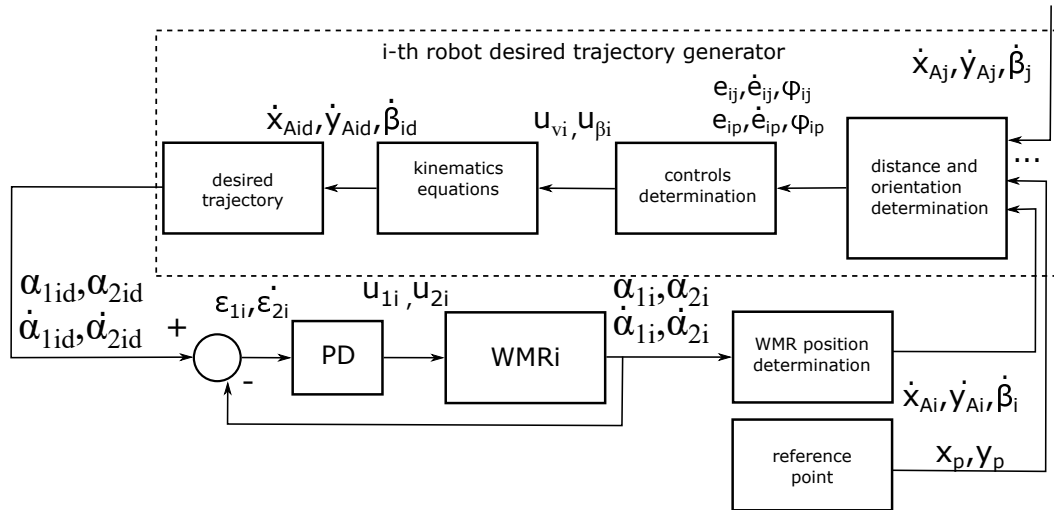


Figure 6. Schematics of swarm self-organization control in case of the  $i$ -th robot

### 3. RESULTS

The simulation and experiment results were obtained for five wheeled robots for the self-organization process. It is assumed that the robots are located around the reference point with known coordinates at a distance not greater than 6 times the desired distance to the reference point. The results are compared with each other using the proposed quality indicator of the self-organization, i.e. the swarm's geometric center.

The closest the coordinates values of the swarm's geometric center to the coordinates of the reference point the higher the quality of the swarm's self-organization. The geometric center of the swarm  $T(x_t, y_t)$  is expressed by (44):

$$x_t = \frac{\sum_{i=1}^n x_{Ai}}{n}, \quad y_t = \frac{\sum_{i=1}^n y_{Ai}}{n}, \quad (44)$$

the velocity of the swarm's geometric center is:

$$\dot{x}_t = \frac{\sum_{i=1}^n \dot{x}_{Ai}}{n}, \quad \dot{y}_t = \frac{\sum_{i=1}^n \dot{y}_{Ai}}{n}, \quad (45)$$

where:  $i$  - robot number,  $n$  - total number of robots.

#### 3.1. Simulation

The task of self-organization of a swarm of wheeled robots is to create a swarm of the desired shape with randomly placed robots around a reference point. Appropriate selection of the distances set by the swarm designer makes it possible to obtain the swarm's shape in the form of a regular polygon. The distances between robots and between robots and the reference point are selected in accordance with the geometric relationships of regular polygons. It is assumed that there are no obstacles. The values of spring and damping coefficients of the virtual spring damper connections as well as the values of the  $\lambda_1, \lambda_2$  parameters are selected experimentally.

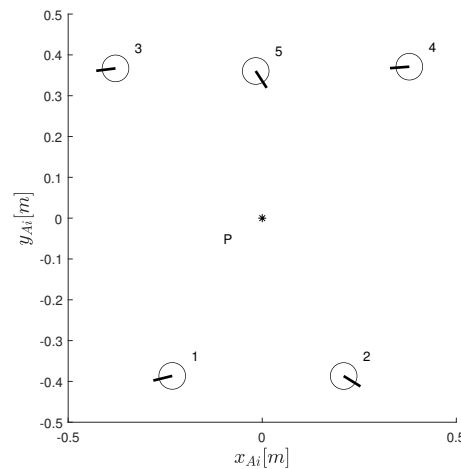
The simulation concerns a swarm of five robots that self-organize around the reference point  $P = [0.0] [m]$ . Initially, the robots are randomly placed around a reference point. Their task is to achieve and maintain the desired distance from each other  $l_{ij}$  and from the reference point  $l_{ip}$ . Due to the introduced sensory disturbances, the figures show the data every twentieth sample. The simulation parameters are presented in the Table 1, while the initial positions of  $A_i$  robots and the frame orientation angles are presented in the Table 2 and in the Figure 7.

Table 1. Assumed parameter values for simulation

No	Parameter	Value
1	$k_{ij}$	0.8[N/m]
2	$c_{ip}$	1.8[Ns/m]
3	$l_{ij}$	0.28[m]
4	$k_{ip}$	0.7[N/m]
5	$\lambda_1$	120[rad/Ns]
6	$l_{ip}$	0.24[m]
7	$c_{ij}$	1.8[Ns/m]
8	$\lambda_2$	1[1/kg]

Table 2. Initial values of the coordinates of the  $A_i$  points and the orientation angles of the robot frames

No	Parameter	Initial Value
1	$x_{01}$	-0.23[m]
2	$y_{01}$	-0.386[m]
3	$\beta_{01}$	-2.91[rad]
4	$x_{04}$	0.378[m]
5	$y_{04}$	0.371[m]
6	$\beta_{04}$	-3.07[rad]
7	$x_{02}$	0.21[m]
8	$y_{02}$	-0.387[m]
9	$\beta_{02}$	-0.53[rad]
10	$x_{05}$	-0.016[m]
11	$y_{05}$	0.36[m]
12	$\beta_{05}$	-0.97[rad]
13	$x_{03}$	-0.378[m]
14	$y_{03}$	0.366[m]
15	$\beta_{03}$	-3.02[rad]

Figure 7. The initial positions of  $A_i$  points and the orientations of the robot frames no. 1-5

In the first stage of self-organization, i.e. the robots' approach to the reference point at a distance close to the desired distance. The inter-robot distances 6-11s, and distance between the robot no. 1 and the reference point as shown in Figure 8 tend to go beyond the setpoints because of the high velocity  $v_{id}$ . The robots correct their positions by moving away from each other until the distances are close to the desired ones. In the second stage of the swarm's movement, i.e. in the stage of correction of the inter-robot distance and the distance to the reference point as shown in Figure 8 11-43s, the distances oscillate around the desired values. This shows that the robots introduce position corrections in relation to each other. The Figure 9 shows the final paths of the robots. Due to the change in the direction of the resultant virtual force acting on the  $i$ -th robot, the robots corrected their position to minimize the value of this force. The effect of minimizing the value of the virtual force are different curves of the robot paths.

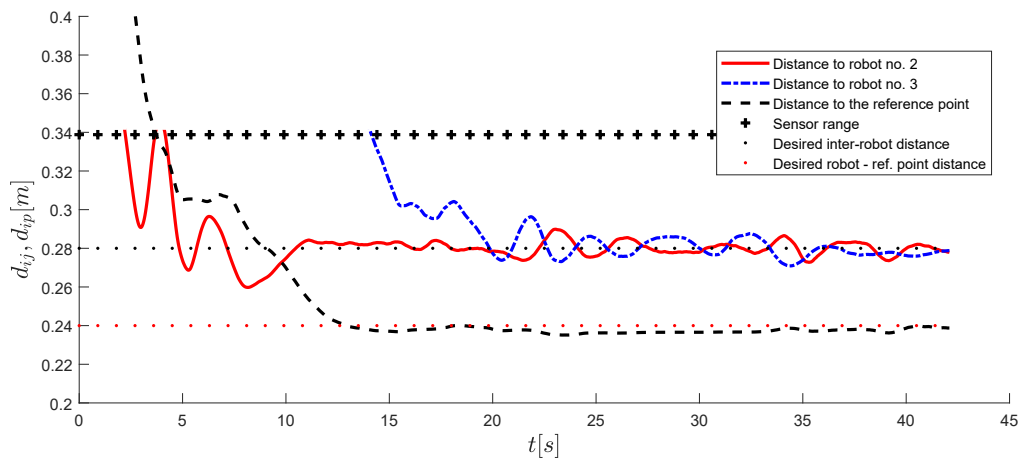


Figure 8. Distances obtained between robot no. 1, the reference point and other neighboring robots in the swarm

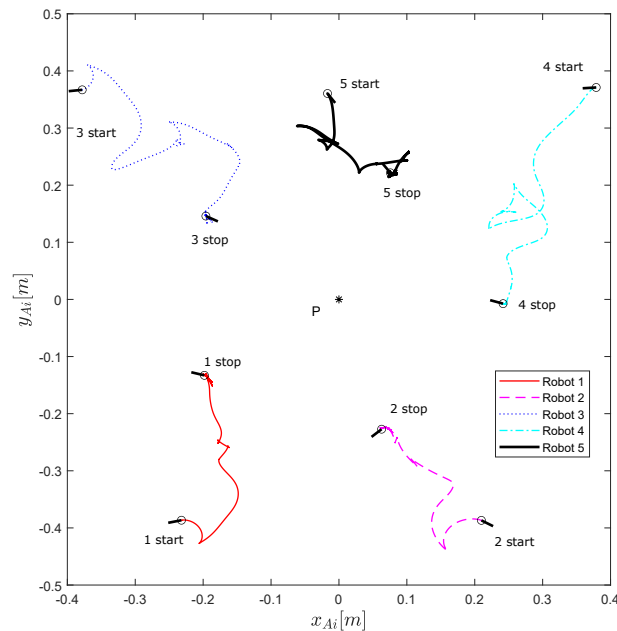


Figure 9. Paths of robots

Figures 10(a) and 10(b) illustrate the geometrical parameters of the swarm movement. In the initial stage of the swarm's movement, the position of the swarm's geometric center differs from the position of the reference point. It is related to the fact that the robots did not reach the desired distance between themselves, which translates into the movement of the robots towards or away from the neighboring robots. As the value of the distance between the robots approaches the value of the desired distance, the force between the robots and the reference point becomes the dominant virtual force, which causes the swarm to move towards it. In the second stage of the swarm's movement, the values of the coordinates of the swarm's geometric center are close to the coordinates of the reference point, oscillating due to the corrections of the distance between the robots. Over the course of the simulation, the coordinates of the geometric center approach the coordinates of the reference point as shown in Figures 10(a) and 10(b). The simulation results show that in the process of self-organization, the robots were able to achieve the desired distance between themselves and the reference point. Assuming that the values of the desired distances between the robots are proportional to the desired distance to the reference point, the swarm reached the shape of a regular pentagon.

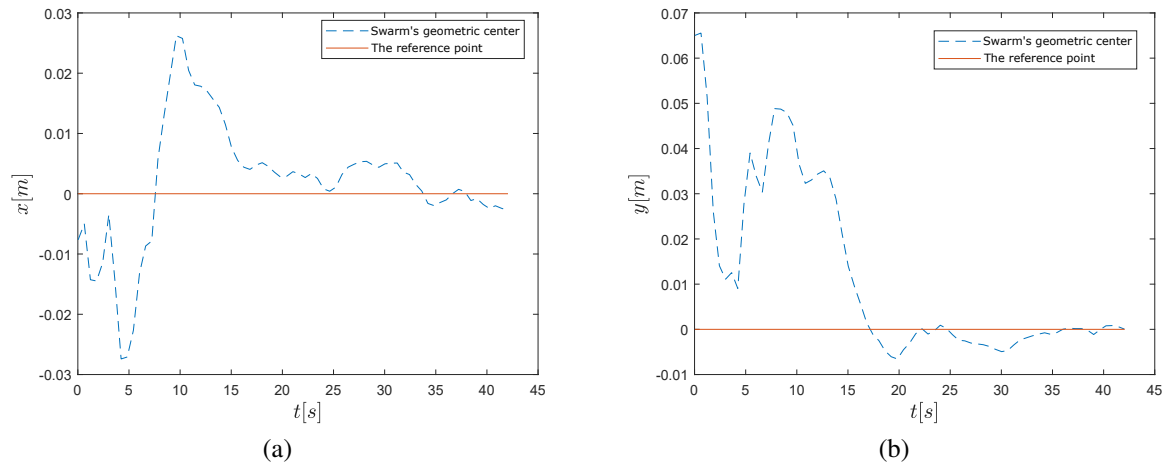


Figure 10. Comparison of the values of the coordinates of the swarm's geometric center and the reference point (a) x coordinates and (b) y coordinates

### 3.2. Experiment

The motion capture system was used to verify the tests. The robotic arena as shown in Figure 11 is used for experimental research and testing algorithms for controlling a swarm or a group of wheeled robots, it consists mainly of two systems: a vision system and a wireless communication system with robots. Motion capture [25] is a technology that allows for determination the position and tracking the movement of markers that reflect or generate infrared light. The technology is based on a vision system consisting of more than three infrared cameras. The experimental research presented in the paper was carried out on a research robotic arena made available by the Federal University of Technology in Lausanne thanks to participation in the The European Robotics Research Infrastructure Network (TerriNet) project. The robotic arena as shown in Figure 11 was equipped with infrared cameras enabling the determination of the position of passive markers placed on the robot as shown in Figure 12 with an accuracy of 0.15 mm while maintaining 350 frames per second . The experiment was carried out for the same values of swarm parameters as in the simulation.



Figure 11. Robotic arena

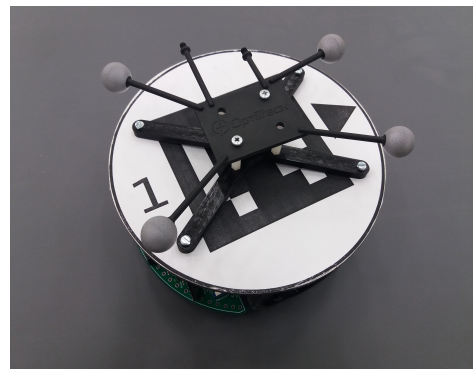


Figure 12. Robotic with markers

Inter-robot distances as shown in Figure 13 over time they achieve a difference of less than  $0.01[m]$  from the desired value. As in the simulation Figure 8, the robots correct their positions by moving away from each other until distances are close to the desired values. The Figures 14(a) and 14(b) show the geometrical parameters of the motion. The coordinates of the geometrical center of the swarm follow the coordinates of the as shown in Figure 14(a) and 14(b), similarly to the simulation. The x and y coordinates of the swarm's geometric center decrease with time and tend to zero oscillating around it. The maximum deviation of coordinates of the swarm's geometric center from the reference point refers to the y coordinate and is equal to  $0.05[m]$ .

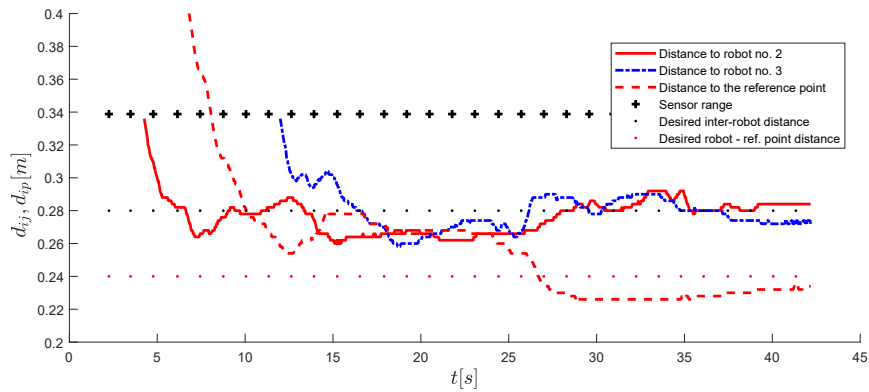
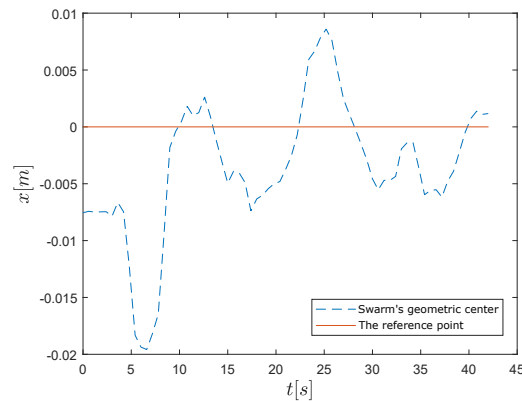
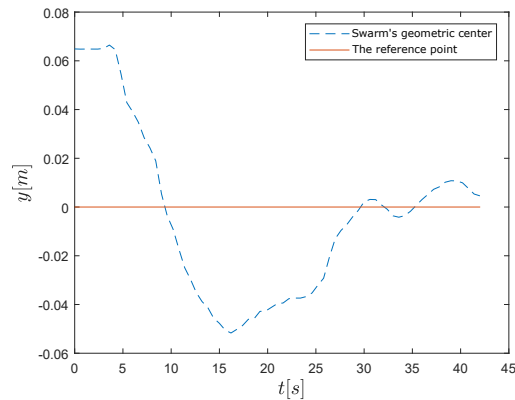


Figure 13. Distances obtained between robot no. 1, the reference point and other neighboring robots in the swarm



(a)



(b)

Figure 14. Comparison of the values of the coordinates of the swarm's geometric center and the reference point (a) x coordinates and (b) y coordinates

Similarly to the Figure 9, the robot paths Figure 15 shows the self-organization of the swarm into the shape of a regular pentagon. Comparing the paths of motion of the robots from the experiment to the simulation results, a similar shape can be noticed. The paths of robot no. 1 are particularly similar to each other. The arrangement of the robots in the final shape of the swarm is similar to the simulation results. Discrepancies may result from inaccuracies in determining the values of the parameters of the swarm mathematical model, in particular the robot dynamics model and disturbances.

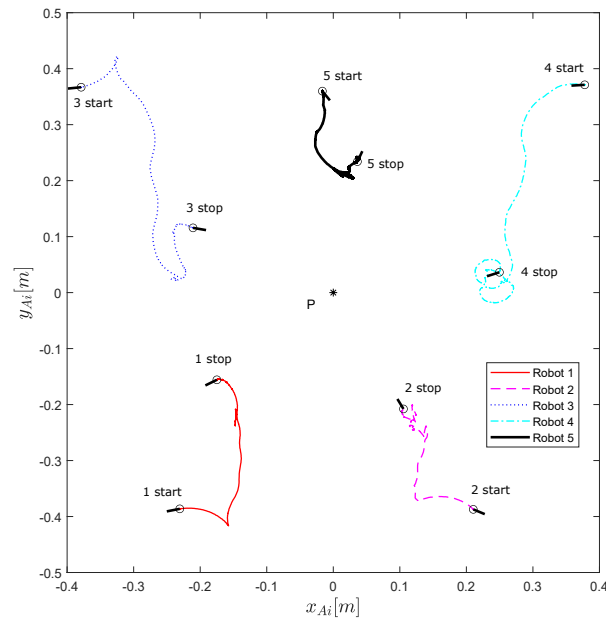


Figure 15. Paths of robots

#### 4. DISCUSSION

The conducted research has shown that a swarm of five randomly placed robots in relation to a given reference point, under the influence of virtual forces from the nearest robots and from a reference point, reaches a shape similar to the desired shape of a regular pentagon. The obtained distances between the closest robots and between the robots and the reference point are close to the desired value. The value of the difference in distance does not exceed 4%. In the initial stage of the swarm's self-organization, the position of the swarm's geometric center differs from the position of the reference point due to the random initial positions of the robots. As the difference in the distance between the robots decreases, the virtual force acting from the reference point becomes the dominant virtual force acting on the robots. This results in faster convergence of the coordinates of the geometric center of the swarm to the coordinates of the reference point.

The experimental studies of the swarm self-organization, show that the achieved distance between the closest robots differed by 0.01 [m] from the set value of 0.28 [m]. The error in reaching the desired distance between the robots and the reference point was also 0.01 [m] for the desired distance equal to 0.24 [m]. The final position of the swarm's geometric center in the case of the simulation and the experiment was similar to the position of the reference point. The distance between the geometric center of the swarm and the reference point was less than 0.01 [m].

#### 5. CONCLUSIONS

The paper presents a method of virtual forces enabling the shape control of a swarm of wheeled robots. The analysis and synthesis of the self-organization algorithm of a swarm of robots is presented. The research concerned the self-organization of the swarm, i.e. the arrangement of robots around a given, stationary reference point, maintaining the given distances between neighboring robots and between the robots and the reference point.

Numerical tests were carried out along with experimental studies of the self-organization tasks. The experiments were carried out on a robotic arena using a motion capture system. Similar results from numerical tests and verification tests were obtained for the proposed control algorithm. The obtained results of the performed numerical tests and experimental tests prove the correctness of the model of a robotic swarm. In the plots of coordinates values and projections of the velocity of the geometric center of the swarm, the stages of acceleration, movement at a steady velocity and deceleration of the swarm can be distinguished. Moreover, based on the simulation and experiment results, it can be concluded that the swarm behaves like an elastically deformable body. The results of the conducted verification coincided with the simulation results. It can con-

cluded that the adopted description of the swarm's behavior is correct and based on the experiment results, the proposed control algorithm enables the self-organization of the swarm into a given regular pentagon shape.

## REFERENCES

- [1] S. Camazine, J.-L. Deneubourg, N. R. Franks, J. Sneyd, G. Theraula, and E. Bonabeau, *Self-organization in biological systems*. Princeton University Press, 2003.
- [2] G. Baldassarre, V. Trianni, M. Bonani, F. Mondada, M. Dorigo, and S. Nolfi, "Self-organized coordinated motion in groups of physically connected robots," *IEEE Transactions on Systems, Man and Cybernetics, Part B (Cybernetics)*, vol. 37, no. 1, pp. 224–239, Feb. 2007, doi: 10.1109/TSMCB.2006.881299.
- [3] C. Ampatzis, E. Tuci, V. Trianni, A. L. Christensen, and M. Dorigo, "Evolving self-assembly in autonomous homogeneous robots: experiments with two physical robots," *Artificial Life*, vol. 15, no. 4, pp. 465–484, Oct. 2009, doi: 10.1162/artl.2009.Ampatzis.013.
- [4] C. Ampatzis, E. Tuci, V. Trianni, A. L. Christensen, and M. Dorigo, "Evolving self-assembly in autonomous homogeneous robots: experiments with two physical robots," *Artificial Life*, vol. 15, no. 4, pp. 465–484, Oct. 2009, doi: 10.1162/artl.2009.Ampatzis.013.
- [5] P. Vincent and I. Rubin, "A framework and analysis for cooperative search using UAV swarms," in *Proceedings of the 2004 ACM Symposium on Applied Computing*, Jan. 2004, doi: 10.1145/967900.967919.
- [6] Y. U. Cao, A. S. Fukunaga, and A. Kahng, "Cooperative mobile robotics: antecedents and directions," *Autonomous Robots*, vol. 4, no. 1, pp. 7–27, 1997, doi: 10.1023/A:1008855018923.
- [7] C. Pinciroli, R. O'Grady, A. Christensen, and M. Dorigo, *Self-organised recruitment in a heterogeneous swarm*. 2009.
- [8] J. D. Hasbach and M. Bennewitz, "The design of self-organizing human–swarm intelligence," *Adaptive Behavior*, vol. 30, no. 4, pp. 361–386, Jul. 2021, doi: 10.1177/10597123211017550.
- [9] B. Zhou, Q. Yang, L. Dou, H. Fang, and J. Chen, "An attempt to self-organized polygon formation control of swarm robots under cyclic topologies," *IFAC-PapersOnLine*, vol. 53, no. 2, pp. 11000–11005, Jan. 2020, doi: 10.1016/j.ifacol.2020.12.024.
- [10] M. C. Thrun and A. Ultsch, "Swarm intelligence for self-organized clustering," *Artificial Intelligence*, vol. 290, Jan. 2021, doi: 10.1016/J.ARTINT.2020.103237.
- [11] W. M. Spears and D. F. Spears, *Physicomimetics: physics-based swarm intelligence*. Berlin, Heidelberg: Springer Berlin Heidelberg, 2012.
- [12] A. E. Turgut, C. Huepe, H. Çelikkanat, F. Gökçe, and E. Şahin, "Modeling phase transition in self-organized mobile robot flocks," in *Ant Colony Optimization and Swarm Intelligence*, M. Dorigo, M. Birattari, C. Blum, M. Clerc, T. Stützle, and A. F. T. Winfield, Eds. Berlin, Heidelberg: Springer Berlin Heidelberg, 2008, pp. 108–119.
- [13] E. Ferrante, A. E. Turgut, N. Mathews, M. Birattari, and M. Dorigo, "Flocking in stationary and non-stationary environments: a novel communication strategy for heading alignment," in *Parallel Problem Solving from Nature, PPSN XI*, Berlin, Heidelberg: Springer Berlin Heidelberg, 2010, pp. 331–340.
- [14] G. Tan, J. Zhuang, J. Zou, L. Wan, and Z. Sun, "Artificial potential field-based swarm finding of the unmanned surface vehicles in the dynamic ocean environment," *International Journal of Advanced Robotic Systems*, vol. 17, no. 3, May 2020, doi: 10.1177/1729881420925309.
- [15] T. Balch and M. Hybinette, "Social potentials for scalable multi-robot formations," in *Proceedings 2000 ICRA. Millennium Conference. IEEE International Conference on Robotics and Automation. Symposia Proceedings (Cat. No. 00CH37065)*, Apr. 2000, vol. 1, pp. 73–80, doi: 10.1109/ROBOT.2000.844042.
- [16] H.-S. Kim, Y.-H. Joo, and J.-B. Park, "Formation control for swarm robots using artificial potential field," *Journal of Korean Institute of Intelligent Systems*, vol. 22, no. 4, pp. 476–480, Aug. 2012, doi: 10.5391/JKIIS.2012.22.4.476.
- [17] D. H. Kim, H. Wang, and S. Shin, "Decentralized control of autonomous swarm systems using artificial potential functions: analytical design guidelines," *Journal of Intelligent and Robotic Systems*, vol. 45, no. 4, pp. 369–394, 2006, doi: 10.1007/s10846-006-9050-8.
- [18] E. Falomir, S. Chaumette, and G. Guerrini, "A mobility model based on improved artificial potential fields for swarms of UAVs," in *2018 IEEE/RSJ International Conference on Intelligent Robots and Systems (IROS)*, Oct. 2018, pp. 8499–8504, doi: 10.1109/IROS.2018.8593738.
- [19] R. Ravindranathan Nair and L. Behera, "Swarm aggregation using artificial potential field and fuzzy sliding mode control with adaptive tuning technique," in *2012 American Control Conference (ACC)*, Jun. 2012, pp. 6184–6189, doi: 10.1109/ACC.2012.6315463.
- [20] R. L. Galvez *et al.*, "Obstacle avoidance algorithm for swarm of quadrotor unmanned aerial vehicle using artificial potential fields," in *TENCON 2017 - 2017 IEEE Region 10 Conference*, Nov. 2017, pp. 2307–2312, doi: 10.1109/TENCON.2017.8228246.
- [21] J. Wiech and V. Eremeyev, "Virtual spring damper method for nonholonomic robotic swarm self-organization and leader following," *Continuum Mechanics and Thermodynamics*, vol. 30, no. 5, 2018, doi: 10.1007/s00161-018-0664-4.

- [22] M. J. Giergiel, Z. Hendzel, and W. Żylski, *Modeling and control of mobile wheeled robots (in Polish)*. PWN Scientific Publishing House, 2013.
- [23] M. W. Spong, S. Hutchinson, and M. Vidyasagar, “Robot modeling and control,” *IEEE Control Systems*, vol. 26, no. 6, pp. 113–115, Dec. 2006, doi: 10.1109/MCS.2006.252815.
- [24] W. Żylski, “Motion planning for wheeled mobile robot using potential field method,” *Journal of Theoretical and Applied Mechanics*, vol. 42, no. 3, pp. 695–705, 2004.
- [25] M. Field, D. Stirling, F. Naghdy, and Z. Pan, “Motion capture in robotics review,” in *2009 IEEE International Conference on Control and Automation*, Dec. 2009, pp. 1697–1702, doi: 10.1109/ICCA.2009.5410185.

## BIOGRAPHIES OF AUTHORS



**Jakub Wiech**     is an Assistant Professor the Department of Applied Mechanics and Robotics at the Rzeszow University of Technology (Poland). He received his Ph.D. in Mechanical Engineering from the Rzeszow University of Technology in 2022. In 2019 he participated in the TerriNet project, working on control algorithms for wheeled robotic swarms. His research interests lie in the field of robotics, especially, autonomous control systems for mobile robots. His research interest also includes mechanical vibrations analysis and machine learning.